Available online at www.sciencedirect.com
SCIENCE DIRECT®
Biochimica et Biophysica Acta 1655 (2004) 248–255
BIOCHIMICA ET BIOPHYSICA ACTA
BBA
www.bba-direct.com

Review

The use of stable isotopes and spectroscopy to investigate the energy transducing function of cytochrome *c* oxidase

Bryan Schmidt[a,b], Warwick Hillier[b], John McCracken[b], Shelagh Ferguson-Miller[a,*]

[a] *Department of Biochemistry and Molecular Biology, Michigan State University, East Lansing, MI 48824, USA*
[b] *Department of Chemistry, Michigan State University, East Lansing, MI 48824, USA*

Received 23 April 2003; received in revised form 5 November 2003; accepted 5 November 2003

Abstract

We have used EPR and FTIR spectroscopy in combination with ^{17}O and ^{15}N stable isotopes to investigate the mechanism of cytochrome *c* oxidase (CcO). A high-spin state of heme a_3 was found in high yield by EPR, achieved upon turning over the enzyme until it was anaerobic, and shown to be a mixture of heme with a coordinated oxygen-based ligand and five-coordinate heme. Allowing the enzyme to consume $^{17}O_2$ for a few milliseconds before freezing, we also showed that the product $H_2^{17}O$ exits toward the external side of the enzyme, binding to the nonredox active Mg/Mn site en route.

Specific ^{15}N labeling of histidine, in comparison with global ^{15}N labeling and unlabeled samples, allowed us to more definitively assign heme and histidine peaks in the electrochemically induced FTIR difference spectrum. Additionally, the assignment of heme bands affords a reliable method of spectrum normalization between samples, providing a more accurate comparison of the spectral features of bovine with bacterial cytochrome oxidase and revealing multiple differences between the two species.

Keywords: Cytochrome aa_3; EPR; FTIR; Stable isotope; Water; Heme

Scientific investigation of the redox enzyme known as cytochrome *c* oxidase (CcO) has a history dating more than 100 years (see Ref. [1]). However, there is still no clear understanding of the specifics of its mechanism. This is not due to lack of brilliant minds working on the problem, but rather to the complexity of its structure and function. CcO spans the lipid bilayer and takes electrons from one side and protons from the other, catalyzing their combination with molecular oxygen at a dimetallic heme/copper site to produce two water molecules (see Ref. [2]). The manner in which this enzyme controls the cleavage of the stable dioxygen bond, while minimizing the release of any toxic intermediates, has been difficult to determine because of the rapidity of the reaction. But even a good understanding of the oxygen chemistry fails to address the fundamental action of this enzyme: how the energy released by the oxygen bond cleavage is utilized in translocating protons across a membrane to create an electrochemical gradient.

The emergence of high-resolution crystal structures of mammalian (bovine heart) [3] and bacterial (*Paracoccus denitrificans*) [4] oxidases in 1995 allowed for a great advance in understanding of CcO activity, but did not reveal the mechanism of how it pumps protons. (As Jerry used to remind us, ‘‘If the question you are asking can be solved by a good crystal structure, you need to be thinking of a different question.’’) Indeed, the crystal structures give little insight into the oxygen chemistry and the conformational dynamics that occur during the reaction cycle, for which additional methods of investigation are needed. The rapid time resolution of modern spectroscopic methods and the abundance of metal centers in CcO (Fig. 1) that give the enzyme its beautiful green color make visible and magnetic spectroscopies the tools of choice in studies of the dynamics of CcO function [5–11]. Yet once again, these methods have limitations: many focus only on the immediate vicinity of the metal cofactors, blind to the bulk of the protein structure, while others that include the whole structure are limited by the ability to make assignments. The combining of spectroscopies and the use of selective stable isotopes allow investigation into the mechanism to go further, to probe the enzyme on a broad scale from

* Corresponding author. Tel.: +1-517-355-0199; Fax: +1-517-353-9334.
E-mail address: fergus20@pilot.msu.edu (S. Ferguson-Miller).

0005-2728/$ - see front matter © 2004 Elsevier B.V. All rights reserved.
doi:10.1016/j.bbabio.2003.11.008

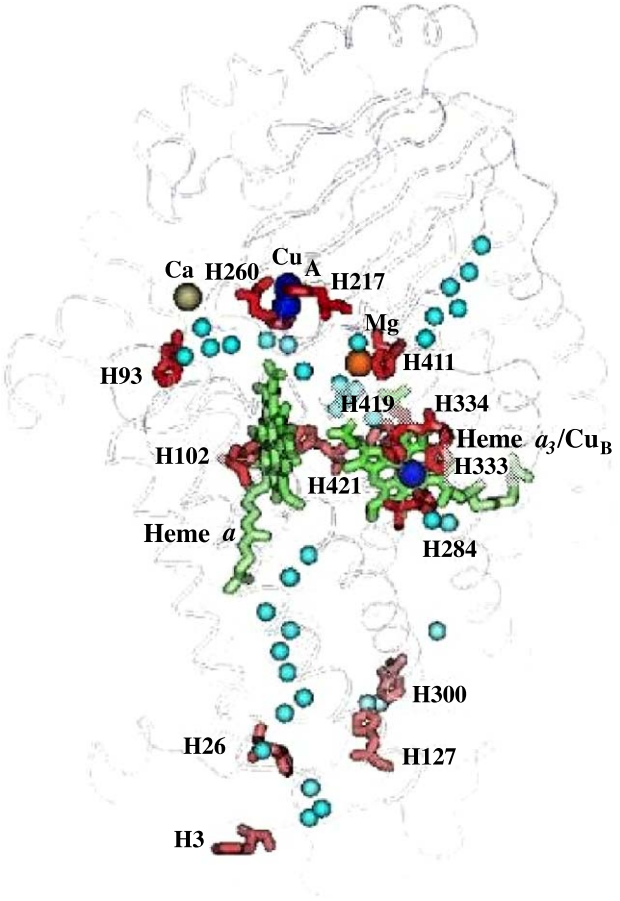

Fig. 1. Essential metal cofactors of bacterial cytochrome *c* oxidase and their protein ligands. There are four redox-active metal centers, the dinuclear copper center Cu_A (blue spheres), hemes *a* and a_3 (both in green), and the mononuclear copper Cu_B (blue sphere). Additionally, there are two other nonredox active metal centers with unknown function, calcium (grey sphere) and magnesium (orange sphere). Also shown are potentially important histidine residues (shown in red), which include the histidine ligands of metals as well as residues found at the entrance of the D channel and the near the K channel and a potentially interesting histidine found on the outside of the enzyme, H93. Important crystallographically defined water molecules are shown (cyan spheres), including the waters that define the D channel, the waters found in the K channel and two potential water exit channels at the top of the molecule that pass the Mg site. The image was created in RasMol using the *R. sphaeroides* crystal structure [26].

specific metal ligands to conformational changes tens of angstroms away from the active site.

1. EPR analysis of CcO

1.1. The heme a_3 EPR spectrum

The paramagnetic 5/2 spin of the high-spin heme a_3 and the 1/2 spin of Cu_B in the oxidized enzyme should make them ideal for study by EPR, but a combination of magnetic dipole and electronic exchange coupling between these two sites renders them both undetectable. This coupling can be broken by the addition of a single electron that can reduce Cu_B to a diamagnetic state, resulting in an EPR-visible heme a_3 signal. This was previously noted in 1976 [5], but the resulting high-spin heme spectrum only accounted for approximately 20% of the heme a_3 and could not be interpreted. We recently discovered that this high-spin a_3 spectrum can be produced with nearly 100% yield, by accidentally adding high levels of reductant to a sample while looking for the effect of Zn inhibition on the EPR spectrum of the Cu_A site [12]. (Jerry always reminded us to look at the entire spectrum: "You don't want to miss something important just because you are not looking for it"). It is still unclear why these conditions reproducibly result in an enzyme with heme a_3 and Cu_A oxidized, and heme *a* and Cu_B reduced, in the presence of a large excess of reductant (Fig. 2). However, it has allowed us to repeat the experiment in the presence of ^2H_2O and $^{17}O_2$, providing insight into the specific structure that gives such a unique spectrum. (As Jerry often said: "Even a blind squirrel finds a nut every once in a while.")

The complicated spectrum seen in Fig. 2 (black trace) is unusual in that there is a substantial deviation from the nearly axial EPR spectrum ($g_\perp = 6.0$, $g_{||} = 2.0$) typical for six-coordinate high-spin Fe^{3+} heme complexes (the peak near $g = 2.0$ is not easily seen, due to overlapping signals from Cu_A and Mn in that region). It is also not representative of the

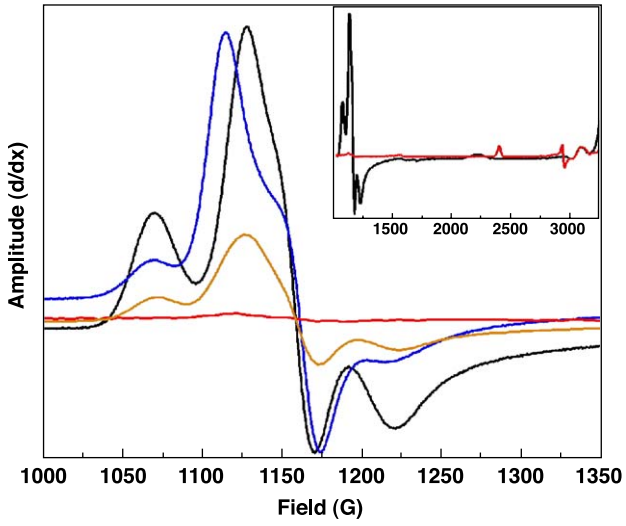

Fig. 2. Six-coordinate ligation of wild-type heme a_3 with an oxygen ligand, shown by ^{17}O broadening. Samples, containing 55 μM CcO, were generated by turning over in oxygenated buffer using 2.4 mM reduced cytochrome *c*, resulting in a majority of heme a_3 visible by EPR (black trace). When prepared in buffer saturated with $^{17}O_2$, the resulting spectrum is broadened, clearly showing the presence of an oxygen ligand that is a product of turnover (blue trace), whereas preparation in deuterated buffer (orange trace) results in a smaller spectrum, indicating protons are required to achieve this state. Inset: Wide scan of the heme a_3 sample, showing heme a_3 and Cu_A spectra consistent with 100% of these metals in the oxidized state but heme *a* completely reduced (black trace), and resting enzyme (red trace), with fully oxidized Cu_A and heme *a* and no heme a_3 or Cu_B observed. Spectra were taken in the perpendicular mode on a Bruker ESP300E spectrometer equipped with a TE112 cavity and maintained at 10 K with an Oxford ESR900 liquid helium flow cryostat.

rhombic EPR spectra typical of five-coordinate high-spin hemes. Instead, this signal must be derived from multiple species, with contributions from both a rhombic species and a more axial species. The center transition is located at $g = 5.95$ and the other two features, which appear to be correlated and give the spectrum its ''pseudo-rhombic shape'', are centered at $g = 6.38$ and $g = 5.60$.

When we attempt to generate high-spin heme a_3 in 80% ^2H_2O-enriched buffer, all the metal cofactors rapidly reduce and a diminished heme a_3 EPR signal is seen (Fig. 2, orange trace). This suggests that protons are involved in achieving this quasi equilibrium state. When instead samples are generated using CcO that has been saturated with $^{17}O_2$, the resulting spectrum has a shifted center transition and the outer features at $g = 6.38$ and $g = 5.60$ are diminished (Fig. 2, blue trace). This demonstrates that there are at least two different components of the spectrum (as postulated by Vänngård [5]), one or more of which is ^{17}O-sensitive. The broadening also demonstrates that there is an oxygen ligand on the heme. It is likely that the spectrum consists of two main components; the rhombic feature, which is broadened by ^{17}O and therefore must have an oxygen-based ligand, and a mostly axial feature, which does not show any noticeable ^{17}O-sensitive broadening at X-band and likely is five-coordinate. Thus, the spectrum in normal buffer is dominated by the rhombic species, with the mostly axial species contributing to give the unusual line shape. When the sample is generated in the presence of $^{17}O_2$, the rhombic feature is broadened, leading to the decreased amplitude of the outer components of the spectrum, while the mostly axial feature is unaltered, resulting in an apparent low-field shift of the center transition.

While no definitive structural assignments can be made yet, there are a limited number of possible states that could account for this spectrum. The presence of the EPR spectrum means the heme a_3 iron must be ferric. Additionally, the spin–spin coupling to Cu_B that is present in resting enzyme must be broken or substantially altered. Since the enzyme does not bind oxygen until heme a_3 is ferrous, and at that point rapidly reacts to become a ferryl-oxo species, the oxygen ligand observed is most likely in the form of either a hydroxyl or a water. The substantial line broadening when produced in the presence of $^{17}O_2$ suggests a tight interaction with the oxygen ligand for the rhombic species and is supported by the unusual degree of rhombicity for a high-spin heme. The lack of evident ^{17}O line broadening and more axial line shape of the center transition suggests this species does not have a tight oxygen ligand and thus is either five-coordinate or has a weakly bound ligand, such as water, as the second axial ligand.

1.2. Product water exit

While the previous experiment observes changes at the redox active metals, we can also investigate the nonredox active Mg site to interrogate the protein away from the active site and closer to the protein surface. Unlike studies on the direct oxygen chemistry that can utilize readily measurable interactions of ligands with the metals, the definition of routes for proton uptake and release, and for substrate water exit, may involve more subtle changes in structure in regions distant from the active site [13–15]. Since these routes could be rate controlling under certain conditions, it is important to define their chemistry and kinetics.

The crystal structures provide some insight into potential proton and water exit routes (Fig. 1), but due to the invisibility of mobile water in crystals, they can offer no definitive answers. Indeed, how does one monitor the movement of individual water molecules in a protein solvated in aqueous buffer? We used the ability of bacterial oxidase to selectively incorporate Mn into the nonredox active Mg site during growth [16] to provide a probe that can detect the movement of water and protons.

The 5/2 electron spin of Mn allowed us to monitor ^2H exchange at the site, demonstrating that the site is readily accessible to bulk [17]. However, it was clear to us that these studies needed to be extended, as they were carried out on resting enzyme and show no proof of the direction of water movement as the enzyme is turning over. The issue of the exit route for product water, generated by the cleavage of molecular oxygen, was addressed by examining CcO that had been rapidly frozen after turning over a few times in buffer saturated by $^{17}O_2$ [18]. Amazingly, extensive broadening of the Mn spectrum was observed, under conditions where a limited number of isotopically labeled waters are produced and the sample is frozen during turnover (Fig. 3).

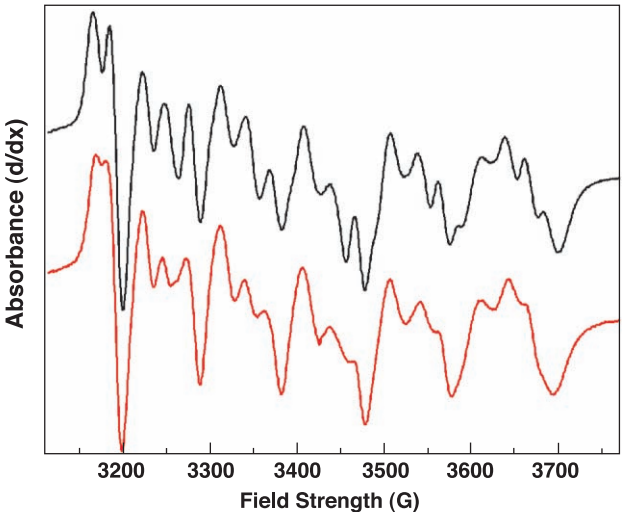

Fig. 3. Mn spectrum of CcO before and after turnover in the presence of 85% $^{17}O_2$ enrichment. Before turnover (no cytochrome *c*, black trace), the sample shows the normal hyperfine structure seen in Mn-enriched CcO. After approximately five turnovers (10 ms with cytochrome *c*, red trace), the sample shows definitive ^{17}O broadening of all hyperfine features, indicating the substantial presence of product water at the Mn. This demonstrates the involvement of the Mn in the product water exit route. Spectra were taken in the perpendicular mode on a Bruker ESP300E spectrometer equipped with a TE112 cavity and maintained at 10 K with an Oxford ESR900 liquid helium flow cryostat.

It was initially a puzzle that a substantial amount of product $H_2^{17}O$ was observed at the Mn^{2+}, since it seems in contradiction to our previous results showing rapid exchange of water with the bulk phase in the same time frame (< 10 ms). However, calculations extrapolated from the number of turnovers completed in 10 ms as measured by cytochrome *c* oxidation in stopped-flow experiments indicate that the turnover of the enzyme would be continuing until the sample was actually frozen. By using a CcO concentration of ~50 μM, an O_2 concentration of 1 mM (saturated at room temperature) and providing electrons, as reduced cytochrome *c*, at ~1 mM, the reaction was limited by reducing equivalents to 5 or fewer complete conversions of O_2 to two H_2O per CcO molecule (four electrons are required to convert one $^{17}O_2$ to two $H_2^{17}O$). Even if all the cytochrome c^{2+} is oxidized, no more than 10 water molecules can be produced per CcO during the reaction time. In fact, under the conditions of this experiment, 10 is an upper limit for $H_2^{17}O$ production, due to the increasing levels of oxidized cytochrome *c* competing with reduced cytochrome *c* causing the rate of turnover to slow down exponentially as the reaction proceeds. Previous stopped-flow kinetic studies, when similarly limited by substrate electrons, suggest that only approximately two complete turnovers would occur within the first 10 ms of the reaction, producing an average of four to six water molecules per CcO and resulting in continued availability of reducing equivalents until the end of the 10 ms before freezing.

Given the level of broadening and the limited number of product waters produced, it is likely that most or all of the waters exit via this route. Thus, the appearance of water at the Mg/Mn site in only a few turnovers argues strongly against the idea that water exits by random diffusion from the active site of CcO, or even by several specific exit routes.

2. FTIR analysis of CcO

2.1. Identification of histidine modes

Histidines are important, often conserved, residues that have been implicated in proton pumping during the turnover of the CcO enzyme. Suggestions that histidine residues may be associated with proton pumping have surfaced because histidine has an almost neutral pK_a (meaning the energetic cost of protonation/deprotonation can be readily met by coupled electron transport) and several of the most highly conserved residues across all species of CcO are histidine. This high degree of conservation of histidines, as well as the favorable pK_a for protonation/deprotonation, was what first led to the proposal that histidine could be essential to the proton pumping mechanism [19,20]. Some mechanisms have been proposed recently that do not explicitly involve histidine as an essential part of the pump [21,22], but the histidine shuttle implies a direct role. Histidines have also been suggested to be essential in other roles, such as the "proton antennae" associated with proton uptake pathways [23].

FTIR spectroscopy can access the involvement of histidine in enzyme turnover from the fully reduced to oxidized state, once specific assignments have been made. We have used global and histidine-specific ^{15}N labeling to make such assignments. Fig. 4 shows the FTIR difference spectra (fully

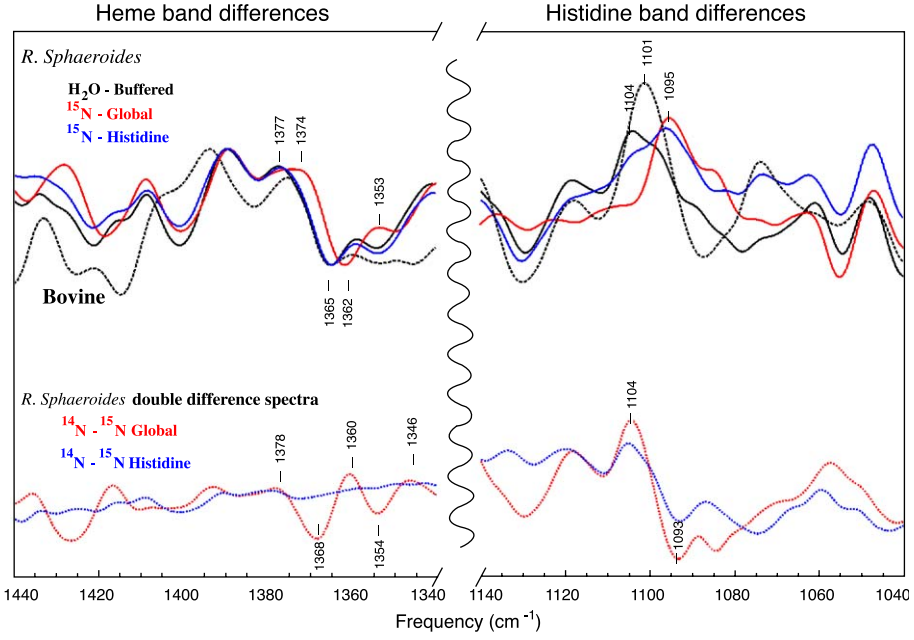

Fig. 4. Electrochemical FTIR difference spectra oxidized–reduced of *R. sphaeroides* cytochrome *c* oxidase, unlabeled (black trace), global ^{15}N globally labeled (red trace), ^{15}N histidine labeled (blue trace), and the bovine CcO (dotted black trace). Double difference spectra for $^{14}N-^{15}N$ (dotted red trace) and $^{14}N-^{15}N$ histidine (dotted blue trace) samples are shown in the lower section. Potentials of +500 mV (oxidized) and −500 mV (reduced) (vs. Ag/AgCl) were used.

oxidized–fully reduced) for the *R. sphaeroides* and bovine oxidases. A positive band at 1104 cm^{-1} is seen in the bacterial system and a band at 1101 cm^{-1} for the mammalian CcO. Model studies suggest that these bands could be associated with histidine [24,25]. To address this question, we isolated CcO enzyme from *R. sphaeroides* cells supplemented with exogenous ^{15}N histidine, as well as cells cultured in $^{15}NH_4Cl$ for global ^{15}N labeling of the whole enzyme. (Following one of Jerry's dictums: "Some problems you can only solve by throwing money at them".)

The spectra from the isolated protein reveals that the 1104 cm^{-1} band undergoes a distinct 9 cm^{-1} down shift as a result of both global ^{15}N labeling and specific ^{15}N ring labeling of the histidine. This 1104 cm^{-1} oxidized feature is the first histidine band definitively assigned in CcO. Furthermore, it appears to be conserved in bacterial and mammalian oxidase enzymes, although it is shifted slightly. Model studies indicate that the band reports on a ν(C5–N1) stretching mode derived from an Nδ protonated histidine [24,25]. Assignment of the residue(s) within the CcO enzyme that correspond to the histidine band is more speculative. The bond could be associated with any of five histidine residues involved in coordinating the redox active hemes a/a_3 or the Cu_B sites (Fig. 1). The third ligand to the Cu_B site, H284, cannot be involved if it is cross-linked to Y288, as is the case in most CcO structures so far examined (but see Ref. [26]). It is also possible that this histidine is not bound to a redox center, but is reporting on protein conformational changes during the four-electron oxidation and reduction of CcO. There exist a number of conserved histidine residues found associated with proton pathways (Fig. 1) that could be altered in their environment or protonation state. Site-specific labeling and mutation experiments need to be performed to make this assignment.

2.2. Heme vibrational bands

The heme vibrational modes in CcO provide important indicators of the oxidation and coordination status of the hemes *a* and a_3, as well as the conformation of the protein in the surrounding area. The heme bands have been widely studied using Raman spectroscopy and indeed Jerry's contributions to the field have been invaluable in determining the structure of the hemes and the nature of the oxygen intermediates [27–30]. However, thus far, the hemes have attracted relatively little interest in FTIR spectroscopy, perhaps because the bands are less easily assigned and overlay protein modes. One FTIR study, using ^{13}C-labeled propionates, has assigned the carboxylate stretching modes of the propionates [31,32], but did not address the other heme modes that do not overlap with the protein modes. Further definitive assignment of FTIR modes would therefore be an important step in interpreting the FTIR spectra of CcO.

To facilitate assignment of heme modes, we have globally labeled CcO from *R. sphaeroides* with ^{15}N-nitrogen. Fig. 4 shows the FTIR difference spectra for the fully oxidized minus reduced CcO. Several bands have apparent changes but notable is a large feature at (+)1377 cm^{-1}, which undergoes a shift to (+)1374cm^{-1} in the global ^{15}N-labeled spectrum, along with a corresponding shift of a negative band at (−)1365 to (−)1362 cm^{-1} and a band (+)1359 to (+)1353 cm^{-1} (the sign of the peak indicating whether it is observed as a peak or a trough in the difference spectrum). Such shifts are indicative of changes in vibrational modes associated with nitrogen but not with histidine, since no change occurs with ^{15}N His labeling. Furthermore, as there is little interaction in this region spectrally from amino acids [33], these bands that shift are prime candidates for assignment to heme.

To further interpret the changes in the 1377–1353 cm^{-1} region, we turned to Raman studies of *a*-type hemes [28,34]. From such studies, spectra have been recorded for both five and six-coordinate ferrous and ferric hemes. One specific pyrrol C–N breathing mode called ν_4 is observed at ~1375 cm^{-1} in oxidized (Fe^{III}) heme and at ~1355 cm^{-1} in the reduced (Fe^{II}) heme [28, 34]. These ν_4 bands are positioned similar to the bands in Fig. 4; however, ν_4 modes are expected to be only weakly FTIR active. Another C–N (out of plane) heme pyrrol mode termed ν_{41} arises from lowered symmetry and should be preferentially detected by FTIR. The ν_{41} band for reduced ferrous heme is found at ~1388–1362 cm^{-1} [28,34], and such changes appear to be similar to the ^{15}N isotope sensitive bands that exhibit shifts in Fig. 4. At present, it is not possible to assign the difference bands in Fig. 4 to a particular mode, i.e., ν_4 or ν_{41}, due to a lack of model compounds. However, the changes to the spectra in the region of 1380–1350 cm^{-1} are consistent with changes upon oxidation and reduction of the heme. The ^{15}N shift of heme bands is also similar to that reported in labeling of the myoglobin (heme *b*) study [35]. One interesting feature apparent in the *double difference* spectrum in the lower part of Fig. 4, i.e., the ^{14}N wild type minus the ^{15}N global labeled enzyme, is the positive and negative features that result from global isotope labeling. Typically, such a double difference spectrum would contain a differential band originating from modes down shifting upon oxidation and upon ^{15}N labeling. The double difference spectrum in Fig. 4, however, appears more complex with contributions arising from more than one band shift and suggests that FTIR heme nitrogen bands are influenced by high-spin/low-spin heme coordination states, i.e., discrete contributions from heme *a* and a_3.

An assignment of a heme mode involving (+)1377, (−)1365, (+)1359, and (−)1353 cm^{-1} bands seems clear based on the ^{15}N shifts. Such ^{15}N shifts do not correlate with other N-modes arising from amide modes or individual amino acids [33] and the corresponding bands are also seen in Fig. 4 from the bovine CcO sample. Previously, heme FTIR bands in the bovine CcO were tentatively assigned, including a 1382 cm^{-1} band attributed to heme a_3 [36]. This band is close to the bands we observe here. In addition, an electrochemical study of *P. denitrificans* CcO made the

tentative heme assignment that ν_{41} bands from the oxidized/reduced heme aa_3 enzyme are at (+)1380/1364 cm^{-1} [37]. These earlier band assignments are in agreement with findings from this work, though not substantiated by ^{15}N labeling. We therefore conclude that heme modes can be assigned in the FTIR spectra of CcO and we plan future experiments using model compounds to discern high- and low-spin heme interactions.

2.3. Bacterial versus mammalian oxidases

The aa_3 CcO family has a number of representatives, the most complex being the mammalian enzyme with 13 subunits, 9 more than the bacterial oxidase. The additional subunits likely have a role in regulation and stability of the enzyme and may be involved in the containment of reactive oxygen intermediates [38]. A question that needs consideration is how similar are the bacterial and mammalian oxidases? A high degree of sequence, spectral, and structural similarity exists, but there may be important differences in substrate delivery and product exit paths. Assessing this is difficult, but can be approached by FTIR comparisons of the global protein conformation between fully oxidized and reduced states. Fig. 5 presents a spectral overlay of the bovine 13-subunit CcO with the *R. sphaeroides* 4-subunit CcO, normalized on the basis of the heme bands assigned above. The overall spectra are very similar, yet several marked discrepancies are also apparent, which point to conformational differences between the proteins. It is conceivable that nonconserved features may provide insight into possible differences in proton pumping pathways or mechanisms.

To consider these differences in more detail, a number of nonconserved bands associated with amide regions are summarized in Table 1. For example, the C=O band (+)1746/(−)1735 cm^{-1} assigned to E286 from bacterial studies [39,40] appears markedly smaller in the bovine CcO, suggesting that molecular changes in that region are different [41]. Another marked change is the (+)1685 cm^{-1} peak in the bovine CcO, which is completely reversed at (−)1684 cm^{-1} in the *R. sphaeroides* enzyme. This feature is suggestive of an alteration in an amide I β-sheet, probably associated with the Cu_A site and regions of subunit II where the most β-sheet structure is found. Other amide I bands around 1676–1671 and 1651–1644 cm^{-1} are also different.

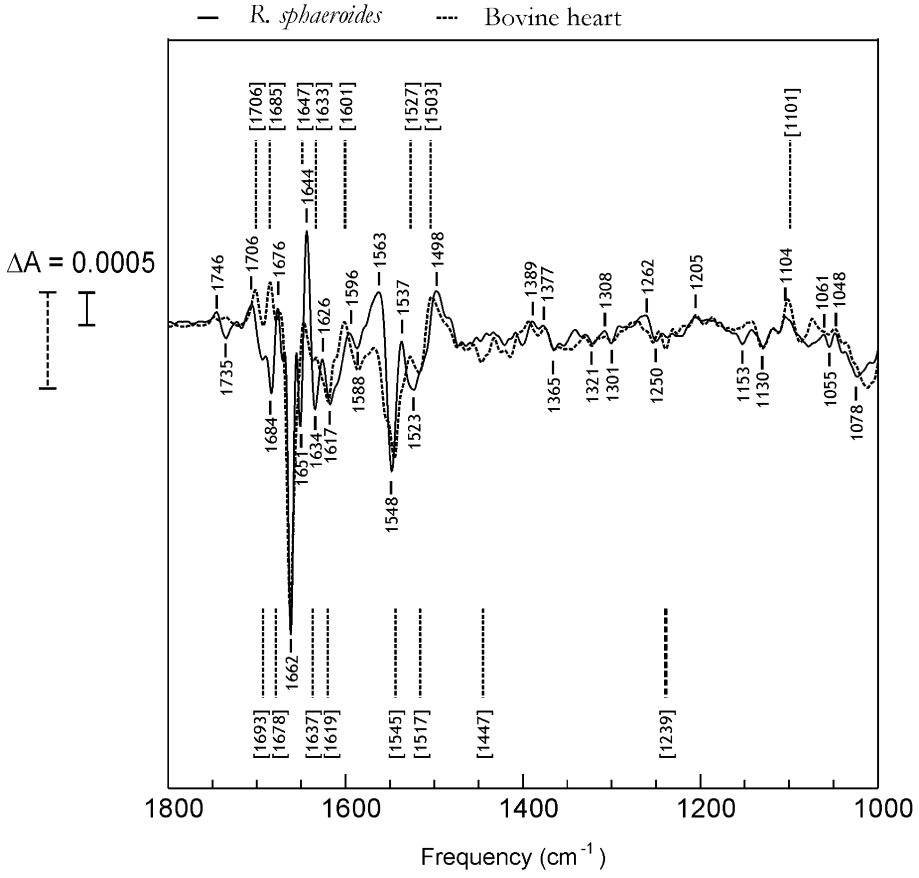

Fig. 5. Electrochemical FTIR difference spectra (oxidized−reduced) of *R. sphaeroides* (solid line) and bovine heart (dashed line) CcO. Potentials of + 500 mV (oxidized) and − 500 mV (reduced) (vs. Ag/AgCl) were used, and to aid spectral comparison the spectra were normalized about the 1389/1365 cm^{-1} heme bands.

Table 1
Nonconserved FTIR difference bands from fully oxidized–fully reduced Cyt. *c* oxidase enzyme

R. sphaeroides	$\Delta(^2H)$	$\Delta(^{15}N)$	Bovine	Assignment
(+)1746	6	1	(+)1748	E(I-286)
(−)1735	5	0	(−)1743	E(I-286)
(+)1706	3	1	(+)1702	ν(C=O) Asp/Glu
(−)1693	–	–	(−)1693	$\nu_{asym}(CN_3H_5^+)$ Arg
(−)1684	0	1		Amide I (β-sheet)
			(+)1685	Amide I (β-sheet)
(+)1676	0	0		Amide I (turns)
			(−)1678	Amide I (turns)
(−)1671	2	1	Absent	Amide I (turns)
(−)1662	0	1	(−)1662	ν(C=O) a/a_3 formyl
(+)1655	1	0	Absent	Amide I (random coil)
(−)1651	0	1	Absent	Amide I (random coil)
(+)1644	1	1	(+)1647	Amide I (β-sheet)
(−)1634	0	1	(−)1644	Amide I (β-sheet)
(+)1626	−2	1	Absent	Amide I (β-sheet)
(−)1617	−3	0	(−)1619	Amide I (β-sheet)
(−)1587	4	2	(−)1586	
(−)1548	0	14	(−)1545	Amide II

These assignments can be compared with that from Refs. [36,37].

One band that we do not see change is at 1588 cm^{-1}. An earlier comparison between the bacterial *P. denitrificans* and the mammalian CcO suggested this (−)1588 cm^{-1} band was only present in the mammalian CcO [42]. It was tentatively assigned as a $\nu_{asym}(COO^-)$ mode from D51 (bovine numbering), a residue not found in the bacterial enzymes. This D51 residue is suggested to be involved in a conformational change linked to proton pumping in the mammalian enzyme [43]; however, comparison of the *R. sphaeroides* with the bovine CcO in Fig. 4 reveals this band at 1588 cm^{-1} in both enzymes.

In summary, there are many changes between the FTIR difference spectra of bacterial and mammalian oxidases. These are of sufficient magnitude to suggest some significant differences in the structural changes associated with the redox chemistry in the two homologous proteins. Thus, analogies between the bacterial and mammalian systems need to be carefully assessed. (As Jerry used to remind us: ‘‘Mother Nature is merciless; she never gives you a break.’’)

3. Conclusions

The use of stable isotopes in combination with FTIR and EPR spectroscopies allows us to look at a variety of detail and dynamics of enzyme function beyond that which can be attained by crystallography alone, or by spectroscopies that only focus on the redox-active hemes. This combination has revealed details of the environment and ligation of the hemes, the movement of product water in the vicinity of a nonredox active metal, and global changes in the protein upon changing of redox states of the metals.

It is apparent from the high-spin heme a_3 spectra, using EPR and $^{17}O_2$, that the enzyme can be trapped with ferric heme a_3 either five-coordinate or with a strong oxygen ligand, in the presence of a large excess of reductant. The product of cytochrome oxidase activity, water, can also be followed by these techniques and is observed to move directionally, not randomly, which may be significant for controlled proton movement.

FTIR with global and histidine-specific ^{15}N labeling reveals local changes within the hemes that depend on the redox states of the metals, allowing us to identify the heme modes. FTIR also reports on more distant structural effects that could be important for the proton pumping mechanism. The incontestable value of bacterial oxidases as model systems for the less manipulable mammalian enzyme must still be viewed with care, given the observed differences in many regions of the FTIR spectra. Nevertheless, it is clear that these spectral and isotope labeling techniques are powerful tools for seeing the minute details of structural change and the big picture of protein dynamics during the catalytic activity of even such a large complex protein as cytochrome *c* oxidase.

Acknowledgements

This work was supported by NIH GM26916 (to SFM), GM37300 (to GTB), GM25486 (to GTB), GM54065 (to JM), PO1 GM57323 (to GTB, JM, SFM), and NIH (RR02231) National Stable Isotope Resource at Los Alamos (which provided the ^{15}N His and $H_2^{17}O$). The authors would additionally like to acknowledge the proprietors of Dagwoods for providing ample beer and an environment that stimulated many discussions that were invaluable to this work.

References

[1] H. Beinert, From indophenol oxidase and atmungsferment to proton pumping cytochrome oxidase aa_3 $Cu_ACu_B(Cu_C?)ZnMg$, Chem. Scr. 28A (1988) 35–40.
[2] S. Ferguson-Miller, G.T. Babcock, Heme/copper terminal oxidases, Chem. Rev. 96 (1996) 2889–2907.
[3] T. Tsukihara, H. Aoyama, E. Yamashita, T. Tomizaki, H. Yamaguchi, K. Shinzawaitoh, R. Nakashima, R. Yaono, S. Yoshikawa, Structures of metal sites of oxidized bovine heart cytochrome *c* oxidase at 2.8 Å, Science 269 (1995) 1069–1074.
[4] S. Iwata, C. Ostermeier, B. Ludwig, H. Michel, Structure at 2.8 Å resolution of cytochrome *c* oxidase from *Paracoccus denitrificans*, Nature 376 (1995) 660–669.
[5] R. Aasa, P.J. Albracht, K.-E. Falk, B. Lanne, T. Vänngård, EPR signals from cytochrome *c* oxidase, Biochim. Biophys. Acta 422 (1976) 260–272.
[6] H. Beinert, R.E. Hansen, C.R. Hartzell, Kinetic studies of cytochrome *c* oxidase by combined EPR and reflectance spectroscopy after rapid freezing, Biochim. Biophys. Acta 423 (1976) 339–355.
[7] G.M. Clore, L.E. Andréasson, B. Karlsson, R. Aasa, B.G. Malmstrom, Characterization of the low-temperature intermediates of the reaction of fully reduced soluble cytochrome oxidase with oxygen by electron paramagnetic resonance and optical spectroscopy, Biochem. J. 185 (1980) 139–154.

[8] P.M. Callahan, G.T. Babcock, Origin of the cytochrome *a* absorption red shift: a pH dependent interaction between its heme *a* formyl and protein in cytochrome oxidase, Biochemistry 22 (1983) 452–461.
[9] G. Antonini, F. Malatesta, P. Sarti, M. Brunori, Proton pumping by cytochrome oxidase as studied by time-resolved stopped-flow spectrophotometry, Proc. Natl. Acad. Sci. U. S. A. 90 (1993) 5949–5953.
[10] I. Szundi, J.A. Cappuccio, N. Borovok, A.B. Kotlyar, Ó. Einarsdóttir, Photoinduced electron transfer in the cytochrome *c*/cytochrome *c* oxidase complex using thiouredopyrenetrisulfonate-labeled cytochrome *c* optical multichannel detection, Biochemistry 40 (2001) 2186–2193.
[11] U. Liebl, G. Lipowski, M. Negrerie, J.C. Lambry, J.L. Martin, M.H. Vos, Coherent reaction dynamics in a bacterial cytochrome *c* oxidase, Nature 401 (1999) 181–184.
[12] D.A. Mills, B. Schmidt, C. Hiser, E. Westley, S. Ferguson-Miller, Membrane potential-controlled inhibition of cytochrome *c* oxidase by zinc, J. Biol. Chem. 277 (2002) 14894–14901.
[13] D.A. Mills, L. Florens, C. Hiser, J. Qian, S. Ferguson-Miller, Where is 'outside' in cytochrome *c* oxidase and how and when do protons get there? Biochim. Biophys. Acta 1458 (2000) 180–187.
[14] D.A. Mills, S. Ferguson-Miller, Proton uptake and release in cytochrome *c* oxidase: separate pathways in time and space? Biochim. Biophys. Acta 1365 (1998) 46–52.
[15] P. Hellwig, B. Rost, W. Mäntele, Redox dependent conformational changes in the mixed valence form of the cytochrome *c* oxidase from *P. denitrificans*: the reorganization of glutamic acid 278 is coupled to the electron transfer from/to heme *a* and the binuclear center, Spectrochim. Acta, Part A: Mol. Biomol. Spectrosc. 57 (2001) 1123–1131.
[16] J.P. Hosler, M.P. Espe, Y.J. Zhen, G.T. Babcock, S. Ferguson-Miller, Analysis of site-directed mutants locates a non-redox-active metal near the active site of cytochrome *c* oxidase of *Rhodobacter sphaeroides*, Biochemistry 34 (1995) 7586–7592.
[17] L. Florens, B. Schmidt, J. McCracken, S. Ferguson-Miller, Fast deuterium access to the buried magnesium/manganese site in cytochrome *c* oxidase, Biochemistry 40 (2001) 7491–7497.
[18] B. Schmidt, J. McCracken, S. Ferguson-Miller, A discrete water exit pathway in the membrane protein cytochrome *c* oxidase, Proc. Natl. Acad. Sci. U. S. A. 100 (2003) 15539–15542.
[19] J.E. Morgan, M.I. Verkhovsky, M. Wikström, The histidine cycle: a new model for proton translocation in the respiratory heme–copper oxidases, J. Bioenerg. Biomembranes 26 (1994) 599–608.
[20] M. Wikström, A. Bogachev, M. Finel, J.E. Morgan, A. Puustinen, M. Raitio, M. Verkhovskaya, M.I. Verkhovsky, Mechanism of proton translocation by the respiratory oxidases: the histidine cycle, Biochim. Biophys. Acta 1187 (1994) 106–111.
[21] H. Michel, Cytochrome *c* oxidase: catalytic cycle and mechanisms of proton pumping—a discussion, Biochemistry 38 (1999) 15129–15140.
[22] N. Capitanio, G. Capitanio, M. Minuto, E. De Nitto, L.L. Palese, P. Nicholls, S. Papa, Coupling of electron transfer with proton transfer at heme *a* and CuA (redox Bohr effects) in cytochrome *c* oxidase. Studies with the carbon monoxide inhibited enzyme, Biochemistry 39 (2000) 6373–6379.
[23] Y. Marantz, E. Nachliel, A. Aagaard, P. Brzezinski, M. Gutman, The proton collecting function of the inner surface of cytochrome *c* oxidase from *Rhodobacter sphaeroides*, Proc. Natl. Acad. Sci. U. S. A. 95 (1998) 8590–8595.
[24] K. Hasegawa, T. Ono, T. Noguchi, Vibrational spectra and Ab initio DFT calculations of 4-methylimidazole and its different protonation forms: infrared and Raman markers of the protonation state of a histidine side chain, J. Phys. Chem., B 104 (2000) 4253–4265.
[25] K. Hasegawa, T. Ono, T. Noguchi, Ab initio density functional theory calculations and vibrational analysis of zinc bound 4-methylimidazole as a model of a histidine ligand in metalloenzymes, J. Phys. Chem., A 106 (2002) 3377–3390.
[26] M. Svensson-Ek, J. Abramson, G. Larsson, S. Tornroth, P. Brzezinski, S. Iwata, The X-ray crystal structures of wild-type and EQ(I-286) mutant cytochrome *c* oxidases from *Rhodobacter sphaeroides*, J. Mol. Biol. 321 (2002) 329–339.
[27] P.M. Callahan, G.T. Babcock, Insights into heme structure from Soret excitation Raman spectroscopy, Biochemistry 20 (1981) 952–958.
[28] G.T. Babcock, in: T.G. Spiro (Ed.), Biological Applications of Raman Spectroscopy, Wiley, New York, 1988, pp. 293–346.
[29] J.P. Shapleigh, J.P. Hosler, M.M.J. Tecklenburg, Y.Y. Kim, G.T. Babcock, R.B. Gennis, S. Ferguson-Miller, Definition of the catalytic site of cytochrome *c* oxidase: specific ligands of heme *a* and the heme a_3–Cu_B center, Proc. Natl. Acad. Sci. U. S. A. 89 (1992) 4786–4790.
[30] D.A. Proshlyakov, M.A. Pressler, G.T. Babcock, Dioxygen activation and bond cleavage by mixed-valence cytochrome *c* oxidase, Proc. Natl. Acad. Sci. U. S. A. 95 (1998) 8020–8025.
[31] J. Behr, P. Hellwig, W. Mäntele, H. Michel, Redox dependent changes at the heme propionates in cytochrome *c* oxidase from *Paracoccus denitrificans*: direct evidence from FTIR difference spectroscopy in combination with heme propionate 13C labeling, Biochemistry 37 (1998) 7400–7406.
[32] J. Behr, H. Michel, W. Mäntele, P. Hellwig, Functional properties of the heme propionates in cytochrome *c* oxidase from *Paracoccus denitrificans*. Evidence from FTIR difference spectroscopy and site-directed mutagenesis, Biochemistry 39 (2000) 1356–1363.
[33] A. Barth, The infrared absorption of amino acid side chains, Prog. Biophys. Mol. Biol. 74 (2000) 141–173.
[34] S. Choi, J.J. Lee, Y.H. Wei, T.G. Spiro, Resonance Raman and electronic spectra of heme *a* complexes and cytochrome oxidase, J. Am. Chem. Soc. 105 (1983) 3692–3707.
[35] S.Z. Hu, K.M. Smith, T.G. Spiro, Assignment of protoheme resonance Raman spectrum by heme labeling in myoglobin, J. Am. Chem. Soc. 118 (1996) 12638–12646.
[36] P.R. Rich, J. Breton, Attenuated total reflection Fourier transform infrared studies of redox changes in bovine cytochrome *c* oxidase: resolution of the redox Fourier transform infrared difference spectrum of heme a_3, Biochemistry 41 (2002) 967–973.
[37] P. Hellwig, S. Grzybek, J. Behr, B. Ludwig, H. Michel, W. Mäntele, Electrochemical and ultraviolet/visible/infrared spectroscopic analysis of heme *a* and a_3 redox reactions in the cytochrome *c* oxidase from *Paracoccus denitrificans*: separation of heme *a* and a_3 contributions and assignment of vibrational modes, Biochemistry 38 (1999) 1685–1694.
[38] B. Ludwig, E. Bender, S. Arnold, M. Huttemann, I. Lee, B. Kadenbach, Cytochrome *c* oxidase and the regulation of oxidative phosphorylation, ChemBioChem 2 (2001) 392–403.
[39] P. Hellwig, J. Behr, C. Ostermeier, O.M.H. Richter, U. Pfitzner, A. Odenwald, B. Ludwig, H. Michel, W. Mäntele, Involvement of glutamic acid 278 in the redox reaction of the cytochrome *c* oxidase from *Paracoccus denitrificans* investigated by FTIR spectroscopy, Biochemistry 37 (1998) 7390–7399.
[40] M. Lübben, A. Prutsch, B. Mamat, K. Gerwert, Electron transfer induces side-chain conformational changes of glutamate-286 from cytochrome bo_3, Biochemistry 38 (1999) 2048–2056.
[41] D. Heitbrink, H. Sigurdson, C. Bolwien, P. Brzezinski, J. Heberle, Transient binding of CO to Cu_B in cytochrome *c* oxidase is dynamically linked to structural changes around a carboxyl group: a time-resolved step-scan Fourier transform infrared investigation, Biophys. J. 82 (2002) 1–10.
[42] P. Helwig, T. Soulimane, G. Buse, W. Mantele, Similarities and dissimilarities in the structure–function relation between the cytochrome *c* oxidase from bovine heart and from *Paracoccus denitrificans* as revealed by FT-IR difference spectroscopy, FEBS Lett. 458 (1999) 83–86.
[43] S. Yoshikawa, K. Shinzawa-Itoh, R. Nakashima, R. Yaono, E. Yamashita, N. Inoue, M. Yao, M.J. Fei, C.P. Libeu, T. Mizushima, H. Yamaguchi, T. Tomizaki, T. Tsukihara, Redox-coupled crystal structural changes in bovine heart cytochrome *c* oxidase, Science 280 (1998) 1723–1729.